COMPUTER-AIDED CIVIL AND INFRASTRUCTURE ENGINEERING

Computer-Aided Civil and Infrastructure Engineering **29** (2014) 279–298

Identification of Instantaneous Modal Parameter of Time-Varying Systems via a Wavelet-Based Approach and Its Application

W. C. Su

National Center for High Performance Computing, Hsinchu, Taiwan

&

C. Y. Liu & C. S. Huang*

National Chiao Tung University, Hsinchu, Taiwan

Abstract: *This work presents an efficient approach using time-varying autoregressive with exogenous input (TVARX) model and a substructure technique to identify the instantaneous modal parameters of a linear time-varying structure and its substructures. The identified instantaneous natural frequencies can be used to identify earthquake damage to a building, including the specific floors that are damaged. An appropriate TVARX model of the dynamic responses of a structure or substructure is established using a basis function expansion and regression approach combined with continuous wavelet transform. The effectiveness of the proposed approach is validated using numerically simulated earthquake responses of a five-storey shear building with time-varying stiffness and damping coefficients. In terms of accuracy in determining the instantaneous modal parameters of a structure from noisy responses, the proposed approach is superior to typical basis function expansion and regression approach. The proposed method is further applied to process the dynamic responses of an eight-storey steel frame in shaking table tests to identify its instantaneous modal parameters and to locate the storeys whose columns yielded under a strong base excitation.*

1 INTRODUCTION

Increased operational loads, design complexity, and building lifetimes of civil, mechanical, and aerospace structures have increased economic and societal demands to monitor the safety of structures against long-term deterioration or under severe loading events such as earthquakes. Early detection of structural degradation is essential for preventing catastrophic failure. A structure under damage typically shows nonlinear dynamical behaviors (Adeli et al., 1978) in which structural stiffness and damping are implicitly dependent on time (Adeli and Jiang, 2006). The time dependence of structural stiffness and damping in a damaged structure results in the instantaneous modal parameters of the structure varying with time. Thus, instantaneous modal parameters of the structure based on its dynamic responses under a single severe loading event can be used to detect whether a structure is damaged and to detect the location of the damage. System identification of structures has been a subject of active research in recent years (Schoefs et al., 2011; Stratman et al., 2011; Marano et al., 2011; Kang et al., 2012; Hazra et al., 2012; Yan and Ren, 2012; Cho et al., 2012; Theodoridis et al., 2012). This research has application in damage detection of structures (Figueiredo et al., 2011;

*To whom correspondence should be addressed. E-mail: *cshuang@mail.nctu.edu.tw*.

DOI: 10.1111/mice.12037

Osornio-Rios et al., 2012; Qiao et al., 2012; Xiang and Liang, 2012; Nishikawa et al., 2012; Raich and Liszkai, 2012), which can then be used for health monitoring of structures (Adeli and Saleh, 1997; Yuen and Katafygiotis, 2006; Park et al., 2007; Moaveni et al., 2009; Bocca et al., 2011; Cusson et al., 2011; Xia et al., 2011; Gangone et al., 2011; Bitaraf et al., 2012) currently a very important area of structural engineering research. The main purposes of this work are to propose an efficient approach for accurately estimating the instantaneous modal parameters of a structure from its dynamic responses and further apply the approach to locate the possible damaged storeys of a building.

The time-varying autoregressive with exogenous input (TVARX) model is often utilized to establish an input–output relationship of a time-varying linear system from its dynamic responses and input forces (Loh et al., 2000; Niedźwiecki, 2000; Jiang and Adeli, 2005, 2007; Jiang et al., 2007; Poulimenos and Fassois, 2006, 2009). However, a continuing challenge is establishing a sufficiently precise TVARX model. Two main classes of approaches have been typically employed to develop the TVARX model, namely, recursive least-squares approach and basis function expansion and regression approach.

Recursive least-squares approach is an online approach that is computationally efficient in estimating time-varying parameters in TVARX model (Ljung and Gunnarsson, 1990; Ljung, 1987). However, the disadvantages in the typical recursive least-squares approach are slow tracking capability for time-varying coefficients and high sensitivity to initial conditions. Proposed techniques for using recursive least-squares approach to minimize such shortcomings include variable forgetting factors (Fortescue et al., 1981; Toplis and Pasupathy, 1988; Leung and So, 2005), covariance matrix resetting (Jiang and Cook, 1992; Park and Jun, 1992), the sliding window technique (Choi and Bien, 1989; Belge and Miller, 2000), the Kalman filter (Loh et al., 2000), and the random walk Kalman filter (Morbidi et al., 2008).

Basis function expansion and regression approach has the advantage of excellent capability on tracking coefficients changing with time. This approach expands the time-varying coefficients of the TVARX model into a finite sequence of predetermined basis functions such as the Fourier series (Marmarelis, 1987), Legendre polynomial (Niedźwiecki, 1988), Walsh function (Zou et al., 2003), wavelets (Tsatsanis and Giannakis, 1993; Adeli and Samant, 2000; Zheng et al., 2001; Karim and Adeli, 2003; Ghosh-Dastidar and Adeli, 2003; Zhou and Adeli, 2003; Jiang and Adeli, 2004; Kim and Adeli, 2005a, b, c; Adeli and Kim, 2004; Adeli and Ghosh-Dastidar, 2004; Ghosh-Dastidar and Adeli, 2006; Adeli et al., 2008; Wei et al., 2010; Li et al., 2011; Lin et al., 2012; Acharya et al., 2012), and shape functions constructed by moving least-squares approach (Huang et al., 2009). In practice, selecting an appropriate set of basis functions is essential for the success of this approach. From a mathematical perspective, however, any complete set of basis functions used to approximate the coefficient functions can obtain a TVARX model with acceptable accuracy as long as the number of basis functions is sufficient. Nevertheless, using high-order polynomials often causes numerical difficulties in an analysis. Numerical experiments by Zou et al. (2003) showed that the Legendre polynomial is effective for coefficients that change smoothly over time, whereas Walsh functions are effective for piecewise stationary time-varying coefficients. To approximate the step-function-type coefficient functions in the TVARX model, Asutkar et al. (2010) demonstrated that Haar basis functions are superior to Cosine and Legendre basis functions. Li et al. (2011) reduced the difficulties on selection of basis function by combining cardinal B-splines wavelet function with a block least mean square or orthogonal least square algorithm, and both rapid and slow variations of time-varying coefficients can be effectively tracked. In a study of a system with a single degree of freedom (DOF), Huang et al. (2009) showed that a set of basis functions consisting of moving least-squares interpolation functions can accurately identify instantaneous modal parameters that smoothly change with time, regardless of whether the change is rapid or slow. Su (2008) further illustrated that the approach of Huang et al. (2009) is reasonably accurate for finding instantaneous modal parameters that are not smooth functions of time.

The literature on structural health monitoring (Cruz and Salgado, 2009; Adewuyi and Wu, 2011; Talebinejad et al., 2011; Jiang et al., 2012) reveals that vibration-based damage detection methods are widely used because they are simple and easily applied. Vibration-based methods typically detect damage based on the modal frequencies, damping ratios, and modal shapes of the overall structure. Most of the vibration-based methodologies reported in the literature require structural data before the damage occurs (reference data) and after the damage occurs. The reference data are often unavailable or difficult to obtain because they are affected by environmental conditions such as temperature (Moser and Moaveni, 2011) and humidity (Wood, 1992). Experimental modal analyses of the Alamosa Canyon Bridge showed that daily temperature change can cause a variation larger than 5% in the estimated fundamental frequency (Sohn et al., 1999). Such environmental effects reduce the reliability of damage identification methods. Therefore, a method is needed to determine whether a building is damaged even when

reference data are unavailable and to identify damage to specific floors of the building based on the dynamic responses of the building to a single severe event such as a strong earthquake.

The proposed approach for using the TVARX model and a substructure technique efficiently identifies the instantaneous modal parameters of a full structure and its substructures. The identified instantaneous modal parameters of an entire building cannot only reveal possible earthquake damage to a building, but also indicate the accuracy of the mathematical model such as finite element model established in design stage if such information is available and modify the model if necessary. Since the identified substructural instantaneous natural frequencies of a building reflect its local behaviors, the frequencies can be further applicable for identifying damage in each floor of the building after an earthquake occurs. An appropriate TVARX model is established by adopting the method of Huang et al. (2009) and continuous wavelet transform to process the dynamic displacement responses of a structure. The proposed approach is validated in a five-storey shear building with time-varying stiffness and damping under base excitation and comparisons with typical basis function expansion and regression approaches using wavelet basis functions. The present approach is further employed to process the measured dynamic displacement responses of an eight-storey steel frame in shaking table tests. Some columns of the frame were observed to yield from the measured strain responses under large base excitation, and the storeys whose columns yielded are exactly located from the substructural instantaneous natural frequencies obtained from the responses of the frame under such large base excitation.

2 METHODOLOGY

A time-varying structural system encountered in civil and mechanical engineering can be described by the following equations of motion:

$$\mathbf{M}\ddot{\mathbf{x}} + \mathbf{C}\dot{\mathbf{x}} + \mathbf{K}\mathbf{x} = \mathbf{f} \tag{1}$$

where **M**, **C,** and **K** are the mass, damping, and stiffness matrices, respectively, and **C** and **K** are the functions of time, while **x** and **f** are displacement and force vectors, respectively. A building may show a nonlinear response to a large earthquake, and its **C** and **K** are implicit functions of time. The instantaneous modal parameters of the building are therefore time-dependent.

The equations of motion in a discrete form are equivalent to

$$\mathbf{y}(t) = \sum_{i=1}^{I} \mathbf{\Phi}_i(t)\mathbf{y}(t-i) + \sum_{j=0}^{J} \mathbf{\Theta}_j(t)\mathbf{f}(t-j) + \mathbf{a}_n(t) \tag{2}$$

where $\mathbf{y}(t-i) \in R^{\bar{n}}$ and $\mathbf{f}(t-i) \in R^{\bar{n}'}$ are the vectors of measured responses and input forces at time $t-i\ \Delta t$, respectively; $1/\Delta t$ is the sampling rate of the measurement, $\mathbf{\Phi}_i(t)$ and $\mathbf{\Theta}_j(t)$ are the matrices of coefficient functions to be determined in the model, and $\mathbf{a}_n(t)$ is a vector representing the residual error accommodating the effects of measurement noise, modeling errors, and unmeasured disturbances. In Equation (2), which is known as the TVARX(I, J) model, the measured displacement responses used for $\mathbf{y}(t-i)$ ensure that the instantaneous modal parameters are directly identifiable from $\mathbf{\Phi}_i(t)$ without systematic error (Huang et al., 2009).

This study combined the method of Huang et al. (2009), who studied a single degree of freedom system, with continuous wavelet transform to estimate the instantaneous modal parameters of a structure. Huang et al. (2009) confirmed that their approach is more efficient than a recursive least-squares technique with variable forgetting factor and a weighted basis function approach (Niedźwiecki, 2000). Here, the use of continuous wavelet transform is proposed for enhancing the accuracy of Huang et al.'s (2009) approach in determining the instantaneous modal parameters of systems with multiple degrees of freedom, especially when processing noisy data.

Each coefficient function in $\mathbf{\Phi}_i(t)$ and $\mathbf{\Theta}_j(t)$ is linearly expanded by the so-called shapes functions constructed through a moving least-squares approach with a set of polynomial basis functions, which is a popular technique in the mesh-free finite-element method (Lancaster and Šalkauskas, 1990; Liu, 2003). The $\phi_{kl}^i(t)$ and $\theta_{kl}^i(t)$, which are (k, l) elements of $\mathbf{\Phi}_i(t)$ and $\mathbf{\Theta}_j(t)$, respectively, can be expressed as

$$\phi_{kl}^i(t) = \boldsymbol{\varphi}(t)\bar{\phi}_{kl}^i \quad \text{and} \quad \theta_{kl}^i(t) = \boldsymbol{\varphi}(t)\bar{\boldsymbol{\vartheta}}_{kl}^i \tag{3}$$

where $\boldsymbol{\varphi}(t) = \mathbf{p}^T(t)\mathbf{A}^{-1}(t)\mathbf{Q}(t)$ is a row vector of shape functions,

$$\mathbf{A}(t) = \sum_{l}^{\bar{l}} w(t, t_l)\mathbf{p}(t_l)\mathbf{p}^T(t_l)$$

$$\mathbf{Q}(t) = [\mathbf{q}_1, \mathbf{q}_2, \ldots, \mathbf{q}_{\bar{l}}]$$

$$\mathbf{q}_l = w(t, t_l)\mathbf{p}(t_l), \quad \mathbf{p}^T = (1, t, t^2, \ldots, t^{\overline{N}})$$

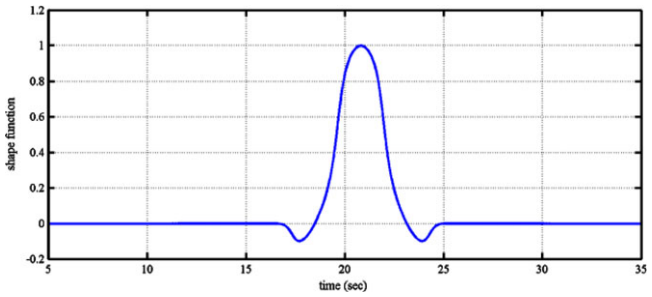

Fig. 1. The shape function corresponding to the node $t = 21$ seconds.

w is a weight function, $\bar{l}$ is the number of nodal points used for each coefficient function, and $\bar{\boldsymbol{\phi}}^i_{kl}$ and $\bar{\boldsymbol{\vartheta}}^i_{kl}$ are two unknown column vectors of coefficients for $\phi^i_{kl}(t)$ and $\theta^i_{kl}(t)$, respectively; $\bar{N}$ denotes the highest order of polynomial in the set of basis functions, $\mathbf{p}$. The derivation of Equation (3) is briefly given in the Appendix. Many weight functions can be used in the above formulation (Liu, 2003). Here, the exponential weight function is used as follows:

$$w(t_m, t_p) = \begin{cases} e^{-((t_m - t_p)/0.3d)^2} & |t_m - t_p|/d \le 1 \\ 0 & |t_m - t_p|/d > 1 \end{cases} \tag{4}$$

where d is the length of the support of the weight function. This weight function is usually used in curve fitting (Lancaster and Šalkauskas, 1990) or constructing shape functions in the mesh-free method (Liu, 2003). According to Huang et al. (2009), who investigated the effects of $\bar{N}$, d, and $\bar{l}$ on the identified instantaneous modal parameters of a single degree of system, this study set $\bar{N} = 2$, $d = 3$ seconds and a nodal point in a second.

Figure 1 shows a typical shape function, which corresponds to node $t = 21$ seconds and is constructed by setting $d = 3$ seconds (in Equation 4) and $\bar{N} = 2$. The shape function is global smooth and vanishes outside a time interval specified by the support of the weight function. A smaller d improves the resulting shape function in expressing better local behaviors of the function to be expanded into the set of such shape functions.

After expanding time-varying coefficients matrices $\boldsymbol{\Phi}_i(t)$ and $\boldsymbol{\Theta}_j(t)$ into a set of shape functions, Equation (2) is rewritten as

$$\mathbf{y}(t) = \sum_{i=1}^{I} \bar{\boldsymbol{\Phi}}_i \boldsymbol{\Gamma}_{i,t} + \sum_{j=0}^{J} \bar{\boldsymbol{\Theta}}_j \boldsymbol{\Pi}_{j,t} + \mathbf{a}_n(t) \tag{5}$$

where

$$\bar{\boldsymbol{\Phi}}_i = \begin{bmatrix} (\bar{\boldsymbol{\varphi}}^i_{11})^T & (\bar{\boldsymbol{\varphi}}^i_{12})^T & \cdots & (\bar{\boldsymbol{\varphi}}^i_{1n})^T \\ (\bar{\boldsymbol{\varphi}}^i_{21})^T & (\bar{\boldsymbol{\varphi}}^i_{22})^T & \cdots & (\bar{\boldsymbol{\varphi}}^i_{2n})^T \\ \vdots & \vdots & \ddots & \vdots \\ (\bar{\boldsymbol{\varphi}}^i_{n1})^T & (\bar{\boldsymbol{\varphi}}^i_{n2})^T & \cdots & (\bar{\boldsymbol{\varphi}}^i_{nn})^T \end{bmatrix},$$

$$\bar{\boldsymbol{\Theta}}_j = \begin{bmatrix} (\bar{\boldsymbol{\vartheta}}^j_{11})^T & (\bar{\boldsymbol{\vartheta}}^j_{12})^T & \cdots & (\bar{\boldsymbol{\vartheta}}^j_{1n'})^T \\ (\bar{\boldsymbol{\vartheta}}^j_{21})^T & (\bar{\boldsymbol{\vartheta}}^j_{22})^T & \cdots & (\bar{\boldsymbol{\vartheta}}^j_{2n'})^T \\ \vdots & \vdots & \ddots & \vdots \\ (\bar{\boldsymbol{\vartheta}}^j_{n1})^T & (\bar{\boldsymbol{\vartheta}}^j_{n1})^T & \cdots & (\bar{\boldsymbol{\vartheta}}^j_{nn'})^T \end{bmatrix}$$

$\boldsymbol{\Gamma}_{i,t} = \mathbf{y}(t-i) \otimes \boldsymbol{\varphi}(t)^{\mathrm{T}}$, $\boldsymbol{\Pi}_{j,t} = \mathbf{f}(t-j) \otimes \boldsymbol{\varphi}(t)^{\mathrm{T}}$, and $\otimes$ denotes Kronecker product. Equation (5) can be treated as a time invariant model with unknown coefficient matrices $\bar{\boldsymbol{\Phi}}_i$ and $\bar{\boldsymbol{\Theta}}_j$.

The above formulations simply extend Huang et al. (2009) to multiple DOF. Conventional least-squares technique is used to find the unknown coefficient matrices $\bar{\boldsymbol{\Phi}}_i$ and $\bar{\boldsymbol{\Theta}}_j$ by minimizing $\mathbf{a}_n^T(t)\mathbf{a}_n(t)$, and this approach is denoted "MLS" approach in the following sections.

It is well known that noise has significant influence in correctly determining $\boldsymbol{\Phi}_i(t)$ and $\boldsymbol{\Theta}_j(t)$ as well as instantaneous modal parameters. Huang and Su (2007) demonstrated that continuous wavelet transform can efficiently reduce the effects of noise in accurately estimating the modal parameters of a linear time invariant system. Consequently, continuous wavelet transform is further introduced into Equation (5). Treating the columns of $\boldsymbol{\Gamma}_{i,t}$ and $\boldsymbol{\Pi}_{j,t}$ as vector functions and applying the continuous wavelet transform to Equation (5) yields

$$W_\psi \mathbf{y}(a,b) = \sum_{i=1}^{I} \bar{\boldsymbol{\Phi}}_i W_\psi \boldsymbol{\Gamma}_{i,(a,b)} + \sum_{j=0}^{J} \bar{\boldsymbol{\Theta}}_j W_\psi \boldsymbol{\Pi}_{j,(a,b)} + W_\psi \mathbf{a}_n(a,b) \tag{6}$$

where the continuous wavelet transform of a function $g(t)$ is defined as

$$W_\psi g(a,b) = \frac{1}{\sqrt{a}} \int_{-\infty}^{\infty} g(t) \psi^* \left(\frac{t-b}{a} \right) dt \tag{7}$$

where the superscript $*$ denotes the complex conjugate; a and b are the scale and translation parameters, respectively; $\psi_{a,b}(t) = (\sqrt{a})^{-1}\psi((t-b)/a)$, and $\psi(t)$ is a mother wavelet function. The translation parameter b is set to $\bar{b}\Delta t$, and $\bar{b}$ is an integer because b must be a

discrete number when the transformation is applied to discrete responses. In the following, $\bar{b}$ is set to 1.

After constructing Equation (6) for different values of a and b, a least-squares approach is applied to determine $\bar{\phi}_{kl}^{i}$ and $\bar{\boldsymbol{\vartheta}}_{kl}^{i}$ by minimizing

$$\bar{E} = \sum_{\bar{m}=1}^{M} \sum_{\bar{n}=1}^{N} [W_\psi \mathbf{a}_n (a_{\bar{m}}, b_{\bar{n}})]^T W_\psi \mathbf{a}_n (a_{\bar{m}}, b_{\bar{n}}) \tag{8}$$

where M and N are the numbers of scale parameters a and data points used in establishing the TVARX model, respectively. The $\bar{\boldsymbol{\phi}}_{kl}^{i}$ and $\bar{\boldsymbol{\vartheta}}_{kl}^{i}$ are then easily obtained by

$$\tilde{\mathbf{C}} = (\mathbf{V}^T \mathbf{V})^{-1} \mathbf{V}^T \tilde{\mathbf{Y}} \tag{9}$$

where

$$\tilde{C} = [\, \bar{\boldsymbol{\Phi}}_1 \quad \bar{\boldsymbol{\Phi}}_2 \quad \cdots \quad \bar{\boldsymbol{\Phi}}_I \quad \bar{\boldsymbol{\Theta}}_0 \quad \bar{\boldsymbol{\Theta}}_1 \quad \cdots \quad \bar{\boldsymbol{\Theta}}_J \,]$$

$$\tilde{\mathbf{Y}} = [\, \tilde{\mathbf{Y}}_{a_1} \quad \tilde{\mathbf{Y}}_{a_2} \quad \cdots \quad \tilde{\mathbf{Y}}_{a_M} \,]$$

$$\tilde{\mathbf{Y}}_{a_{\bar{m}}} = [\, W_\psi \mathbf{y}(a_{\bar{m}}, b_1) \;\; W_\psi \mathbf{y}(a_{\bar{m}}, b_2) \;\; \cdots \;\; W_\psi \mathbf{y}(a_{\bar{m}}, b_N) \,]$$

$$\mathbf{V} = [\, \mathbf{V}_{a_1} \quad \mathbf{V}_{a_2} \quad \cdots \quad \mathbf{V}_{a_M} \,]$$

$$\mathbf{V}_{a_{\bar{m}}} = \begin{bmatrix} W_\psi \boldsymbol{\Gamma}_{1,(a_{\bar{m}},b_1)} & W_\psi \boldsymbol{\Gamma}_{1,(a_{\bar{m}},b_2)} & \cdots & W_\psi \boldsymbol{\Gamma}_{1,(a_{\bar{m}},b_N)} \\ W_\psi \boldsymbol{\Gamma}_{2,(a_{\bar{m}},b_1)} & W_\psi \boldsymbol{\Gamma}_{2,(a_{\bar{m}},b_2)} & \cdots & W_\psi \boldsymbol{\Gamma}_{2,(a_{\bar{m}},b_N)} \\ \vdots & \vdots & \ddots & \vdots \\ W_\psi \boldsymbol{\Gamma}_{I,(a_{\bar{m}},b_1)} & W_\psi \boldsymbol{\Gamma}_{I,(a_{\bar{m}},b_2)} & \cdots & W_\psi \boldsymbol{\Gamma}_{I,(a_{\bar{m}},b_N)} \\ W_\psi \boldsymbol{\Pi}_{0,(a_{\bar{m}},b_1)} & W_\psi \boldsymbol{\Pi}_{0,(a_{\bar{m}},b_2)} & \cdots & W_\psi \boldsymbol{\Pi}_{0,(a_{\bar{m}},b_N)} \\ W_\psi \boldsymbol{\Pi}_{1,(a_{\bar{m}},b_1)} & W_\psi \boldsymbol{\Pi}_{1,(a_{\bar{m}},b_2)} & \cdots & W_\psi \boldsymbol{\Pi}_{1,(a_{\bar{m}},b_N)} \\ \vdots & \vdots & \ddots & \vdots \\ W_\psi \boldsymbol{\Pi}_{J,(a_{\bar{m}},b_1)} & W_\psi \boldsymbol{\Pi}_{J,(a_{\bar{m}},b_2)} & \cdots & W_\psi \boldsymbol{\Pi}_{J,(a_{\bar{m}},b_N)} \end{bmatrix}$$

If only one value of a is used to establish Equation (9), the responses $\mathbf{y}(t)$, $\Gamma_{i,t}$, and $\Pi_{j,t}$ within a certain frequency range are used to find the time-varying coefficients in the TVARX model. The frequency range is determined by the mother wavelet function and the chosen scale parameter. For considering a wide frequency range of responses $\mathbf{y}(t)$, $\Gamma_{i,t}$, and $\Pi_{j,t}$, several values of a can be entered in Equation (9).

After determining $\bar{\boldsymbol{\phi}}_{kl}^{i}$ and substituting them into Equation (3), the coefficient matrices $\boldsymbol{\Phi}_i(t)$ are obtained. Similar to the procedure of obtaining modal parameters from an ARX model (Huang, 2001), a matrix $[\mathbf{G}]$ is constructed from $\boldsymbol{\Phi}_i(t)$ as follows:

$$[\mathbf{G}] = \begin{bmatrix} \mathbf{0} & \mathbf{I} & \mathbf{0} & \cdots & \mathbf{0} \\ \mathbf{0} & \mathbf{0} & \mathbf{I} & \cdots & \mathbf{0} \\ \vdots & \vdots & \vdots & \ddots & \vdots \\ \mathbf{0} & \mathbf{0} & \mathbf{0} & \cdots & \mathbf{I} \\ \Phi_I(t) & \Phi_{I-1}(t) & \Phi_{I-2}(t) & \cdots & \Phi_1(t) \end{bmatrix} \tag{10}$$

where $\mathbf{0}$ is a zero matrix and $\mathbf{I}$ is an identity matrix. Instantaneous modal parameters (natural frequencies, damping ratios, and mode shapes) of the structure can then be estimated from the instantaneous eigenvalues and eigenvectors of $[\mathbf{G}]$. Let $\lambda_k(t)$ and $\{\phi_k(t)\}$ represent the kth eigenvalue and eigenvector of $[\mathbf{G}]$ at time t, respectively. Eigenvalue $\lambda_k(t)$, which is normally a complex function, is set to $\tilde{a}_k(t) + i\tilde{b}_k(t)$. The instantaneous frequency and damping ratio of the system are computed, respectively, by

$$\omega_k(t) = \sqrt{\alpha_k^2(t) + \beta_k^2(t)}, \quad \xi_k(t) = -\alpha_k(t)/\omega_k(t)$$

where

$$\beta_k(t) = \frac{1}{\Delta t} \tan^{-1}\left[\frac{\tilde{b}_k(t)}{\tilde{a}_k(t)}\right],$$

$$\alpha_k(t) = \frac{1}{2\Delta t} \ln\left[\tilde{a}_k^2(t) + \tilde{b}_k^2(t)\right]$$

The procedure developed by Huang (2001) for time invariant systems can then be used to determine the kth instantaneous mode shape.

As a brief summary, the procedure of estimating instantaneous modal parameters from the measured displacement responses of a time-varying system is as follows:

(1) Set the parameters $\bar{l}$, $\bar{N}$, and d in constructing shape functions for the coefficient functions in a TVARX model.
(2) Choose I and J for TVARX(I,J).
(3) Set the appropriate values of a in continuous wavelet transform.
(4) Follow Equations (3)–(6), construct Equation (9) and determine $\bar{\boldsymbol{\phi}}_{kl}^{i}$.
(5) Find $\phi_{kl}^{i}(t)$ from Equation (3) and construct $\boldsymbol{\Phi}_i(t)$.
(6) Determine eigenvalues and eigenvectors of $[\mathbf{G}]$ in Equation (10) and estimate instantaneous modal parameters.

Notably, the whole process must be gone through for some values of I and J, and the accurate modal parameters are determined from the stabilization diagrams for modal parameters. In Step (3), the appropriate values

of a can be roughly determined from the wavelet power spectra of measured responses. They can also be determined from the ranges of the instantaneous natural frequencies estimated roughly by using several values of a to cover a wide range of frequencies.

3 VERIFICATION AND COMPARISON

Numerical simulation responses for a five-storey shear building were processed to confirm the accuracy and effectiveness of the proposed approach in determining instantaneous modal parameters of the building, especially for noisy responses. The material properties of the five-storey shear building are

$$m_i = 0.25 \text{ ton} \quad \text{for } i = 1 \sim 5 \tag{11a}$$

$$\begin{cases} c_1 = 600\left[1 + 0.2\sin\left(\dfrac{\pi t}{5}\right)\right] \text{N}\cdot\text{sec/m} \\ c_i = 300 \text{N}\cdot\text{sec/m} \quad (\text{for } i = 2 \text{ and } 3) \\ c_i = 300\left[1 + 0.2\sin\left(\dfrac{\pi t}{5}\right)\right] \text{N}\cdot\text{sec/m} \\ \qquad (\text{for } i = 4 \text{ and } 5) \end{cases} \tag{11b}$$

$$\begin{cases} k_i = 80\left[1 - 0.2\sin\left(\dfrac{\pi t}{5}\right)\right] \text{kN/m} \\ \qquad (\text{for } i = 1, 4 \text{ and } 5) \\ k_i = 80 \text{ kN/m} \quad (\text{for } i = 2 \text{ and } 3) \end{cases} \tag{11c}$$

where subscript "i" indicates the ith floor or storey. The material properties of the first, fourth, and fifth storeys are periodic functions of time. Notably, periodic functions were often used for the coefficient functions in a TVARX or TVAR model to verify the efficiency of the approaches in published papers (i.e., Niedźwiecki, 2000; Zheng et al., 2001; Li et al., 2011). The Runge–Kutta method gave the dynamic responses of Equation (1) for time increments (Δt) of 0.001 second. The responses and base excitation with $\Delta t = 0.001$ second were resampled with $\Delta t = 0.01$ second for further analyses to identify modal parameters. Figure 2 gives the time histories of base excitation and displacement responses at the second and fifth floors.

Huang et al. (2009) showed that a TVARX model constructed using velocity or acceleration responses produces systematic errors when identifying instantaneous natural frequencies and damping ratios and that the size of the error depends on the change rates of stiffness and damping of the structure under consideration. For this reason, the displacement responses of the five storeys and the input base excitation during 5–35 seconds (see Figure 2) were used to establish TVARX(2,1) models. The TVARX models were constructed using four different approaches: the proposed approach and typical basis function expansion and regression approaches with three different sets of basis functions. The three sets of functions were "db2" and "db4" wavelets (Daubechies wavelets with vanishing moments 2 and 4, respectively) (Daubechies, 1988, 1992) and shape functions constructed by the moving least-squares technique (simply denoted as "db2" and "db4" and MLS approaches, respectively). Notably, these basis function expansion and regression approaches shared the same analysis procedure except that different sets of functions were used to expand the coefficient matrices in the TVARX model.

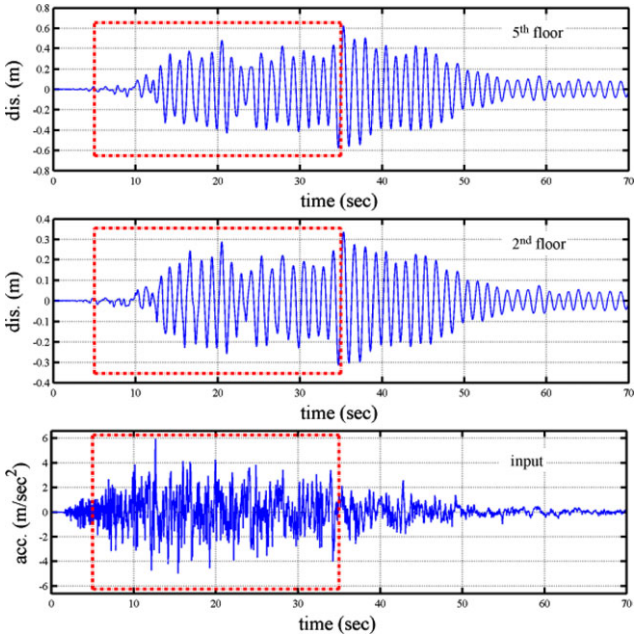

Fig. 2. Time histories of base excitation and simulated displacement responses of the second and fifth floors.

Figure 3 compares the identified instantaneous natural frequencies and modal damping ratios obtained by the proposed approach and by the MLS approach. The support of the weight function (d in Equation 4) and the number of nodal points ($\bar{l}$ in Equation 3) are 3 seconds and 31, respectively. The nodal points are uniformly distributed for t = 5–35 seconds. The continuous wavelet transform in the present approach was carried out using Meyer wavelet function with scale parameters $a = (3/5)^0$, $(3/5)^1$, $(3/5)^2$, $(3/5)^3$, and $(3/5)^4$. Figure 4 plots the Fourier transform modulus of the Meyer wavelet. The figure clearly shows that the Meyer wavelet is not an ideal bandpass filter. If the preserved frequency

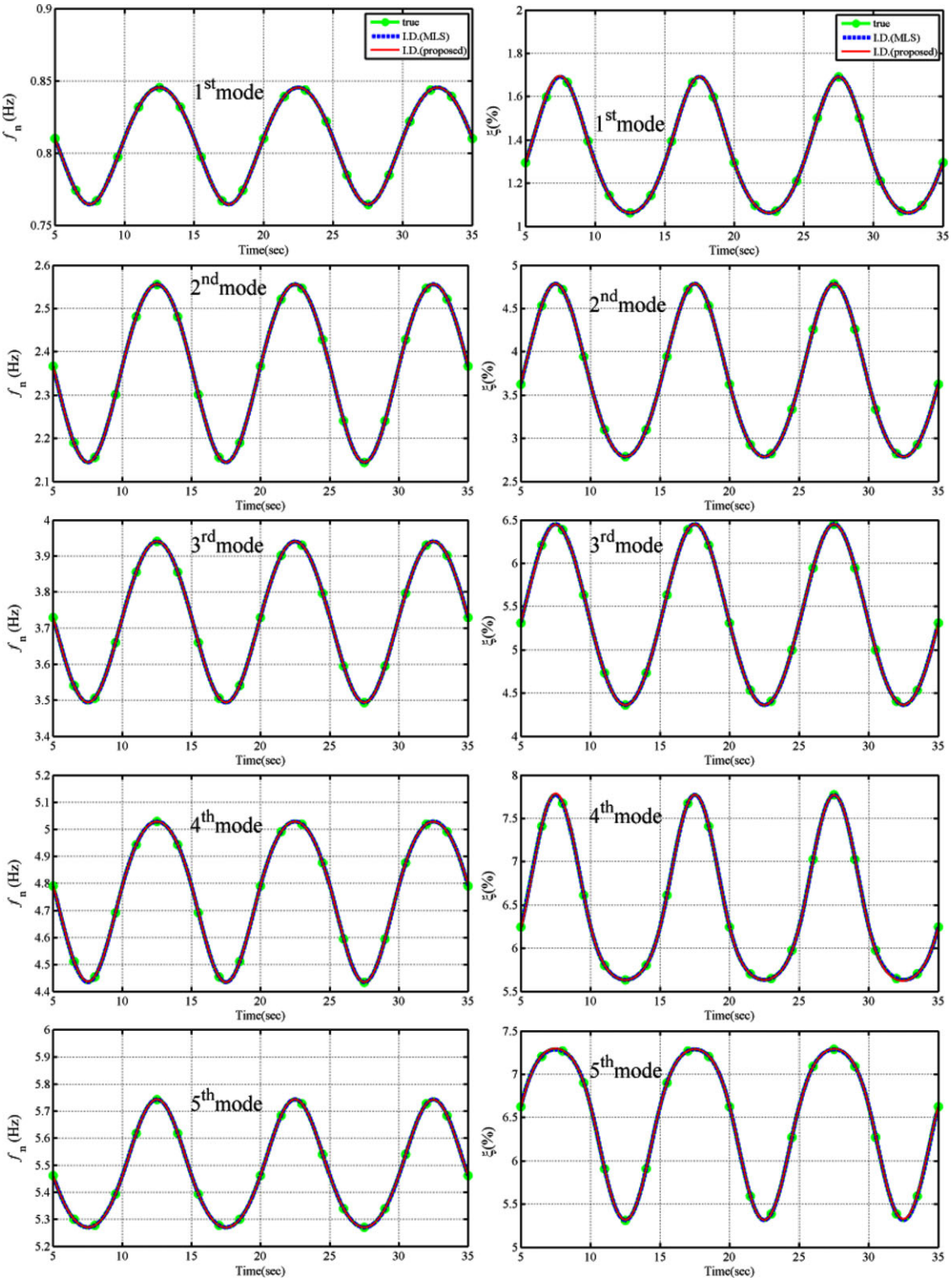

Fig. 3. Instantaneous modal parameters identified from responses without noise via "MLS" and the proposed approaches.

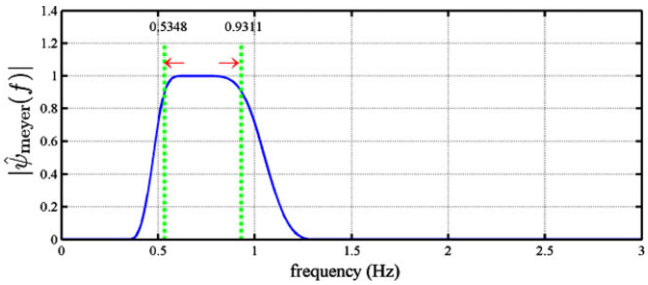

Fig. 4. The Fourier transform modulus of Meyer wavelet.

range for the wavelet is defined simply as the frequency interval in which the Fourier transform modulus of the wavelet exceeds 90% of its maximum value, the Meyer wavelet has the preserved frequency range [0.5348/a, 0.9311/a]. Consequently, when $a = (3/5)^0$, $(3/5)^1$, $(3/5)^2$, $(3/5)^3$, and $(3/5)^4$ are used, $W_\psi \mathbf{y}(a,b)$, $W_\psi \mathbf{\Gamma}_{i,(a,b)}$, and $W_\psi \mathbf{\Pi}_{j,(a,b)}$ in Equation (6) mainly contain the contents in the frequency range of [0.5149, 7.1844] Hz, so the instantaneous natural frequencies in this range should be accurately identifiable. Figure 3 indicates that the identified results by the present approach and MLS approach are highly consistent with the actual values.

Figure 5 gives the identified instantaneous natural frequencies and modal damping ratios obtained by the "db2" and "db4" approaches, which expand each coefficient function in the TVARX model into the following set of wavelet functions:

$$\{\tilde{\phi}_{a,b_1}(t)\ \tilde{\phi}_{a,b_2}(t)\cdots\tilde{\phi}_{a,b_N}(t)\ \psi_{a,b_1}(t)\ \psi_{a,b_2}(t)\cdots\psi_{a,b_N}(t)\}$$

where $\tilde{\phi}_{a,b_i}(t) = 1/\sqrt{a}\tilde{\phi}((t-b_i)/a)$, $\psi_{a,b_i}(t) = 1/\sqrt{a}\psi((t-b_i)/a)$, $\psi(t)$, and $\tilde{\phi}(t)$ are a mother wavelet function (here, a "db2" or "db4" wavelet function) and the corresponding scale function, respectively. In the analyses, the scale and translation parameters were set to $a = 1$ and $b_i = i$(sec), respectively, and $N = 30$. The identified results for "db4" are consistent with the actual values, while the results for "db2" are less accurate than those for "db4." The maximum differences between results obtained from "db2" and the actual values are approximately 2% and 10% in the instantaneous natural frequencies and damping ratios, respectively. Therefore, the discontinuous and fractured "db2" wavelets are unsuitable for expanding the smooth time-varying functions considered here.

In reality, measured responses always contain some level of corrupted noise. To simulate this fact, independent Gaussian white noise with a 5% variance of the noise-to-signal ratio (NSR) was randomly added to the computed displacement responses of five DOFs and the base excitation input. Figure 6 displays the instantaneous natural frequencies and modal damping ratios identified from these noisy data when using the same approaches used to obtain the results in Figures 3 and 5. Since Figures 3 and 5 showed that the worst identification results were obtained when using "db2" basis functions, Figure 6 excludes the results for "db2" basis functions. Other than the order of the TVARX model, all parameters applicable in Figure 6 are identical to those in Figures 3 and 5. The instantaneous modal parameters plotted in Figure 6 were determined from the stabilization diagrams, as shown in Figure 7, which displays the variations of the identified frequencies with the orders of TVARX model and shows the stable appearances of the real mechanical frequencies in different orders of TVARX model.

As expected, the agreement between the identified results and the true values shown in Figure 6 is not as good as that in Figures 3 and 5 due to noise effects. Notably, the instantaneous frequencies and damping ratios of the third to fifth modes and those of the fourth and fifth modes were not completely identified by the "db4" and MLS approaches, respectively, and they are therefore not given in Figure 6. Apparently, Figure 6 reveals that the present approach is substantially superior to the typical basis function expansion approaches with "db4" basis functions and shape functions constructed by moving least-squares technique. The present identified instantaneous natural frequencies and modal damping ratios are different from the exact values by less than 2% and 20%, respectively.

To further demonstrate the capability of the present approach in dealing with noisy responses, Figure 8 depicts the identified instantaneous natural frequencies and modal damping ratios obtained from the noisy responses and input with NSR = 10%. As expected, the agreement between the identified results and true values is a little bit worse than that shown in Figure 6 for the case with NSR = 5%. Nevertheless, the differences between the identified instantaneous natural frequencies and modal damping ratios and the exact values are still less than 2% and 20%, respectively.

4 APPLICATION TO SHAKING TABLE TESTS

To validate the applicability of the proposed approach when using actual measurement, the responses of an eight-storey symmetrical steel frame were measured in shaking table tests (see Figure 9). Shaking table tests are vital to understand the dynamical behaviors, especially nonlinear behaviors, of structures under earthquakes. The eight-storey steel frame analyzed in this test was 1.8 m long, 1.2 m wide, and 8.5 m high (see Figure 9). Lead plates were piled on each floor such that the total mass of steel frame was approximately

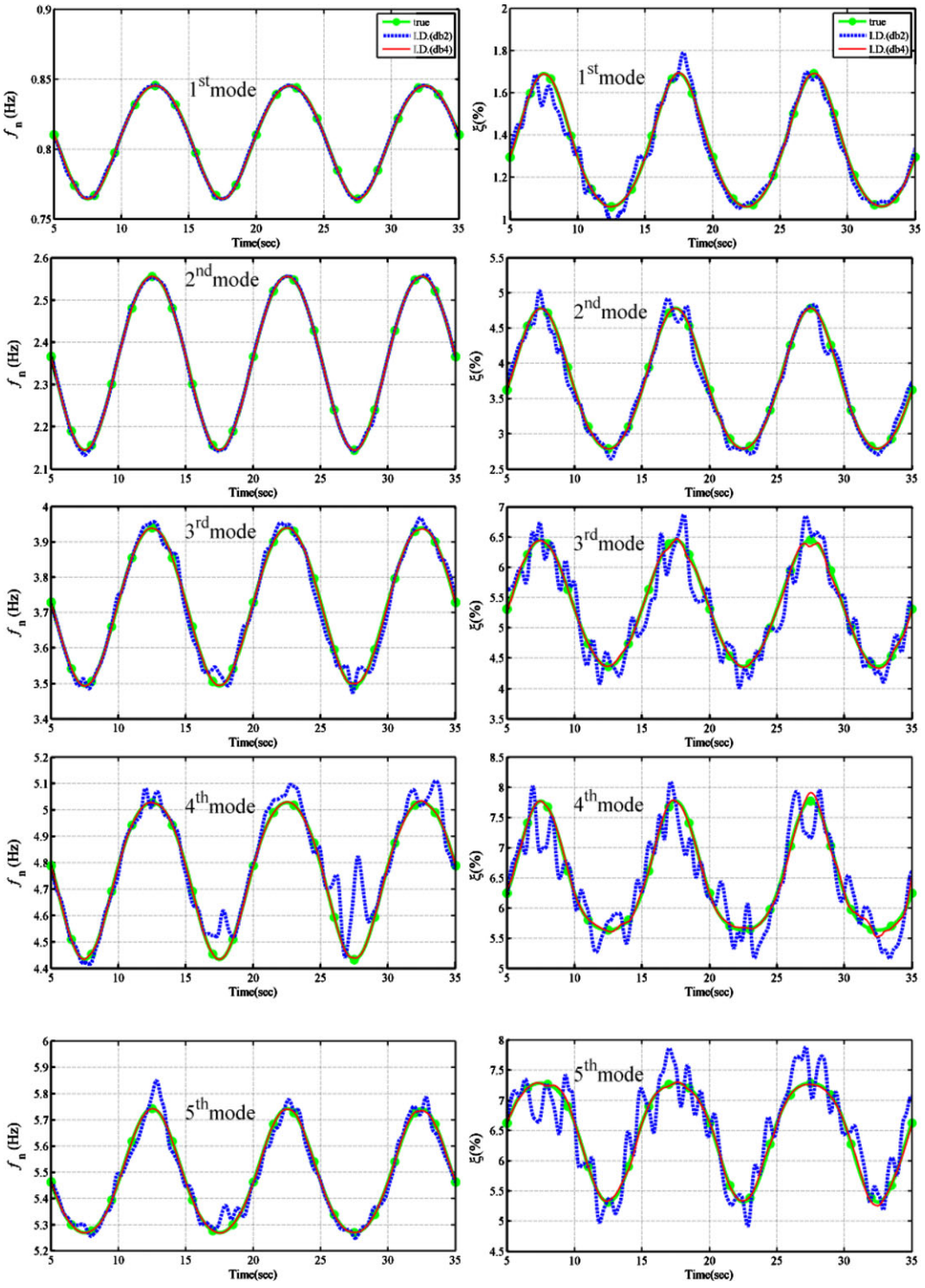

Fig. 5. Instantaneous modal parameters identified from responses without noise via "db2" and "db4" basis functions.

4,519 kg. The columns of the first and third storeys were formed from steel plates with cutoff shown in Figure 10, and the others are formed from intact steel plates.

In the shaking table tests, two accelerometers and two linear displacement transducers were installed in the long-span direction on the two edges of each floor to measure acceleration and displacement responses of the

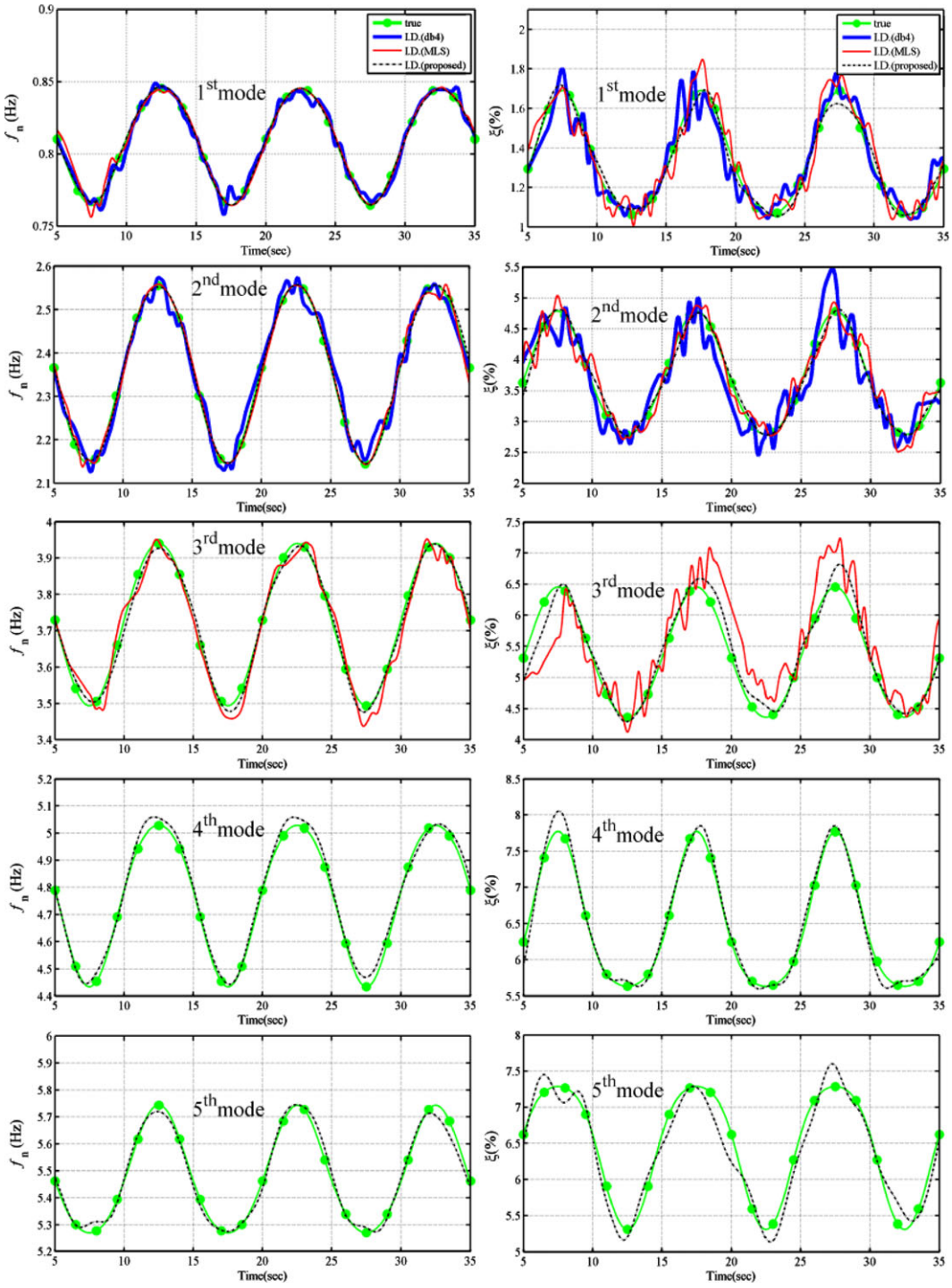

Fig. 6. Instantaneous modal parameters identified from noisy responses (NSR = 5%).

floors, respectively. The average measured responses of the two accelerometers at the base and two displacement transducers on each floor were used in the following analyses. Strain gauges were also installed on one of the four columns in each of the first, second, and third storeys to measure the time history of axial strains. The frame was subjected to base excitations of the 1999 Chi-Chi earthquake, which occurred on September 21, 1999 in Chi-Chi, Nantou County, Taiwan, with different reduced levels, which include 500 gal (5 m/s^2) and 1,200 gal of base excitation levels. Data were recorded at a sampling rate of 200 Hz. Both the acceleration

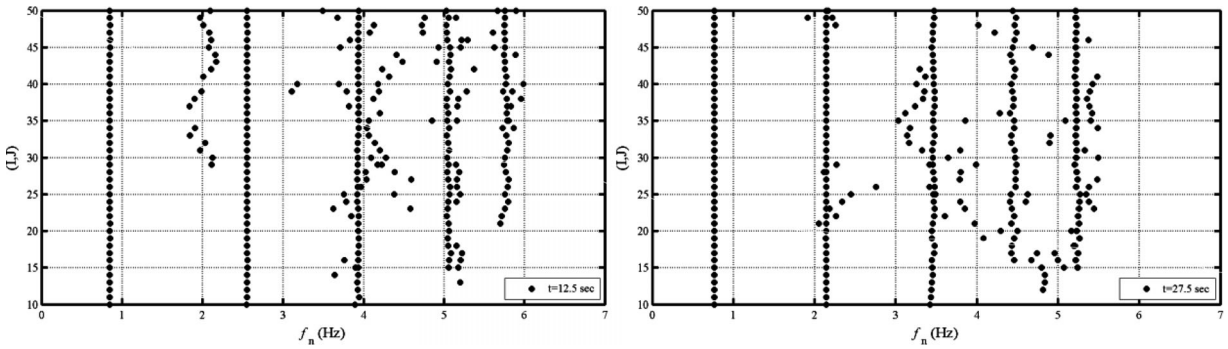

Fig. 7. Identified instantaneous natural frequencies varying with the order of TVARX models at $t = 12.5$ (seconds) and $t = 27.5$ (seconds).

responses of the base and the displacements of all floors at $t = 5$–35 seconds were used in evaluating instantaneous modal parameters of the frame. Figure 11 displays the base excitations and the displacement responses of the first, third, fifth, and seventh floors in the long-span direction of the frame, subjected to 1,200 gal of the 1999 Chi-Chi earthquake. The strain records shown in Figure 12 for different levels of earthquake input confirm that the columns of the first to third storeys yielded when the frame was subjected to 1,200 gal base excitation.

Figure 13 shows the variations of the identified instantaneous natural frequencies and modal damping ratios of eight modes with time for the steel frame under 500 and 1,200 gal of the Chi-Chi earthquake. Since the frame is a symmetric frame with eight storeys, it is expected to have eight vibration modes in the long-span direction of the frame. Theoretically, the natural frequencies and modal damping ratios should be constants since no nonlinear behaviors were observed for the frame under 500 gal base excitation. Figure 13 indeed reveals that, under 500 gal base excitation, variation in the identified natural frequencies over time is lower than 0.01%, and the variations of the identified damping ratios with time are also minor. Figure 13 also illustrates that under 1,200 gal base excitation, highly significant variations of instantaneous natural frequencies and damping ratios with time occur. The minimum natural frequencies and maximum damping ratios for some modes happen at approximately $t = 12$ seconds, which is the approximate time when maximum strains occur (see Figure 12).

5 APPLICATION FOR LOCATING DAMAGED FLOORS OF A SHEAR BUILDING

Sections 3 and 4 have validated the capabilities of the present approach in accurately identifying the instantaneous modal parameters of a structure. The accurately identified instantaneous modal parameters can be employed to determine whether or not the structure has been damaged after a severe earthquake. These identified results can be further used to locate the damaged members or storeys of the structure by applying vibration-based damage detection methods for time invariant systems, e.g., frequency response curvature function method (Sampaio et al., 1999) and flexibility-based methods (Pandey & Biswas, 1994; Patjawit and Knaok-Nukulchai, 2005; Gao et al., 2007). Here, the proposed approach is combined with the substructural approach developed by Su et al. (2012) for time invariant systems to locate the floors of a shear building that are damaged after a severe earthquake.

For most buildings, the assumptions of rigid floors and three DOFs (two horizontal displacement components and one torsion angle) are valid for describing horizontal motion in each floor during an earthquake. In a symmetrical building, the horizontal displacement components and torsion angle of each floor are uncoupled. In this case, its behavior resembles that of a shear building subjected to an earthquake along its symmetric plane.

A shear building with n DOFs is easily decomposed into substructures that have two or three DOFs. If the jth substructure is defined as having $j-1$th, jth, and $j+1$th DOFs (or floors) when $j \neq n$ and $j \neq 1$, then the first substructure is associated with the first and second DOFs, while the nth substructure has the $(n-1)$th and nth DOFs. The following equations in terms of relative acceleration, velocity, and displacement of two floors can be developed:

$$m_n\ddot{x}_n^r + c_n\dot{x}_n^r + k_n x_n^r = f_n - m_n\ddot{x}_{n-1} \quad \text{for } j = n \tag{12a}$$

$$m_j\ddot{x}_j^r + c_j\dot{x}_j^r + k_j x_j^r = f_j - m_j\ddot{x}_{j-1} + c_{j+1}\dot{x}_{j+1}^r + k_{j+1}x_{j+1}^r \quad \text{for } j = 2 \sim (n-1) \tag{12b}$$

$$m_1\ddot{x}_1 + c_1\dot{x}_1 + k_1 x_1 = f_1 + c_2\dot{x}_2^r + k_2 x_2^r \quad \text{for } j = 1 \tag{12c}$$

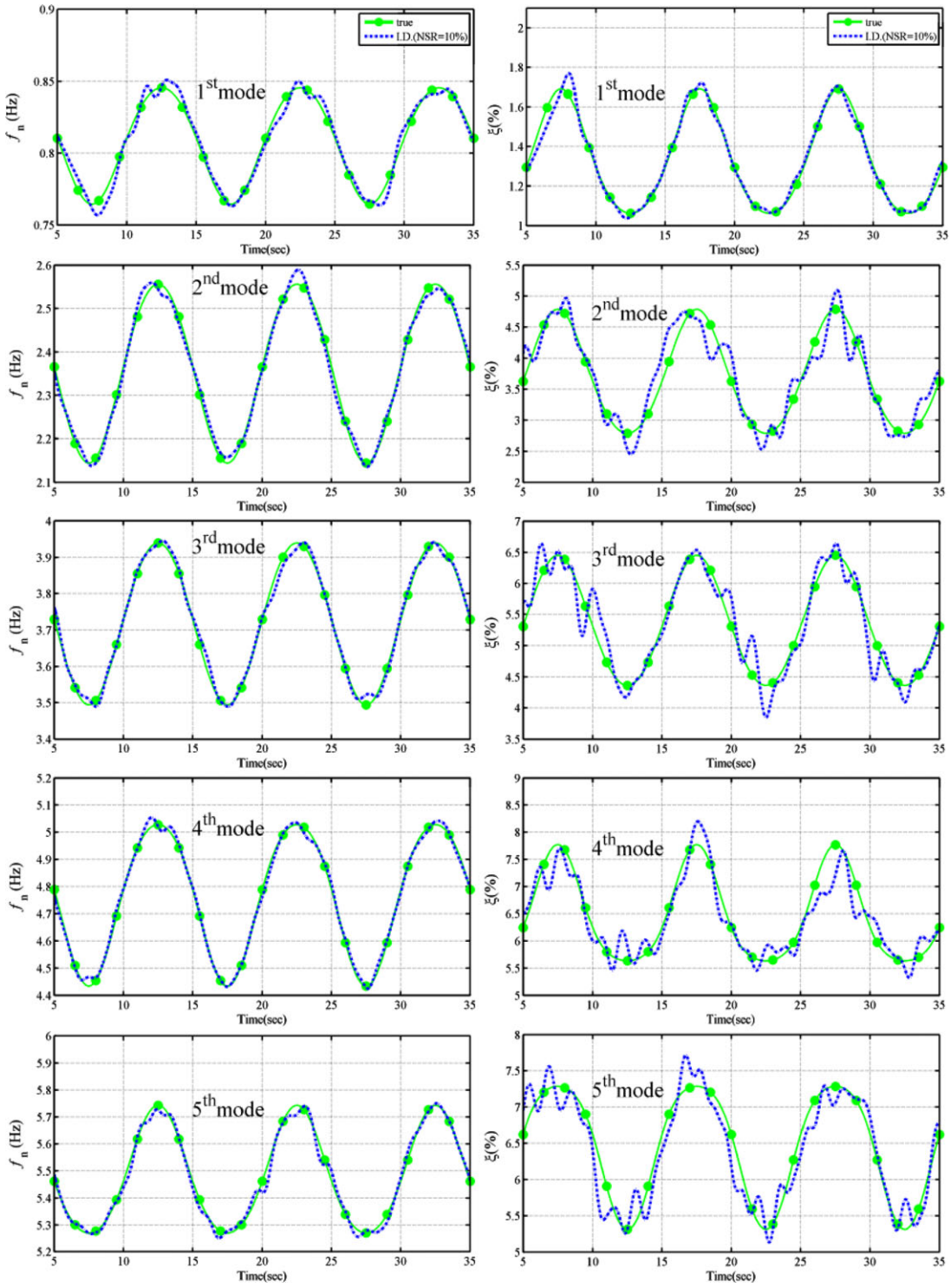

Fig. 8. Instantaneous modal parameters identified from noisy responses (NSR = 10%).

where $x_j^r = x_j - x_{j-1}$. If a multiple input/single output (MISO) TVARX model with output of x_j^r and inputs of f_j ($= -m_j a_g$, and a_g is base excitation acceleration), x_{j-1} and x_{j+1}^r for each $j = 2$ to $(n-1)$, then the instantaneous natural frequency of the jth substructure (storey), which is theoretically $\sqrt{k_j(t)/m_j}$ (Hz), should be obtainable. Similarly, MISO TVARX models can be established for the first and nth substructures.

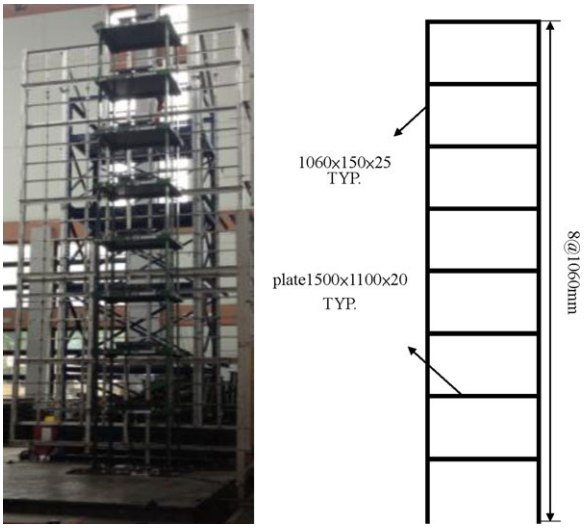

Fig. 9. Photograph and simple sketch of eight-storey frame.

Fig. 10. A photograph of a steel plate with cutoff.

Notably, Su et al. (2012) demonstrated that an ARX model constructed by using x_j^r as output and f_j, x_{j-1} and x_{j+1}^r as inputs for $j = (n-1)$ may not be exactly equivalent to Equation (12b) in a linear time invariant system. This observation also applies to a linear time-varying system. Hence, the procedure proposed by Su et al. (2012) for identifying the natural frequency of the $(n-1)$th substructure in a linear time invariant system is simply extended to the linear time-varying system herein. A multiple input/multiple output (MIMO) TVARX model for $(n-1)$th and nth storeys are constructed with outputs of x_n and x_{n-1} and inputs of a_g and x_{n-2}. The established MIMO gives two instantaneous natural frequencies $\omega_1(t)$ and $\omega_2(t)$ (rad/s), which are related to material properties of $(n-1)$th and nth storeys by

$$\omega_1\omega_2 = \sqrt{\frac{k_{n-1}k_n}{m_{n-1}m_n}} \tag{13}$$

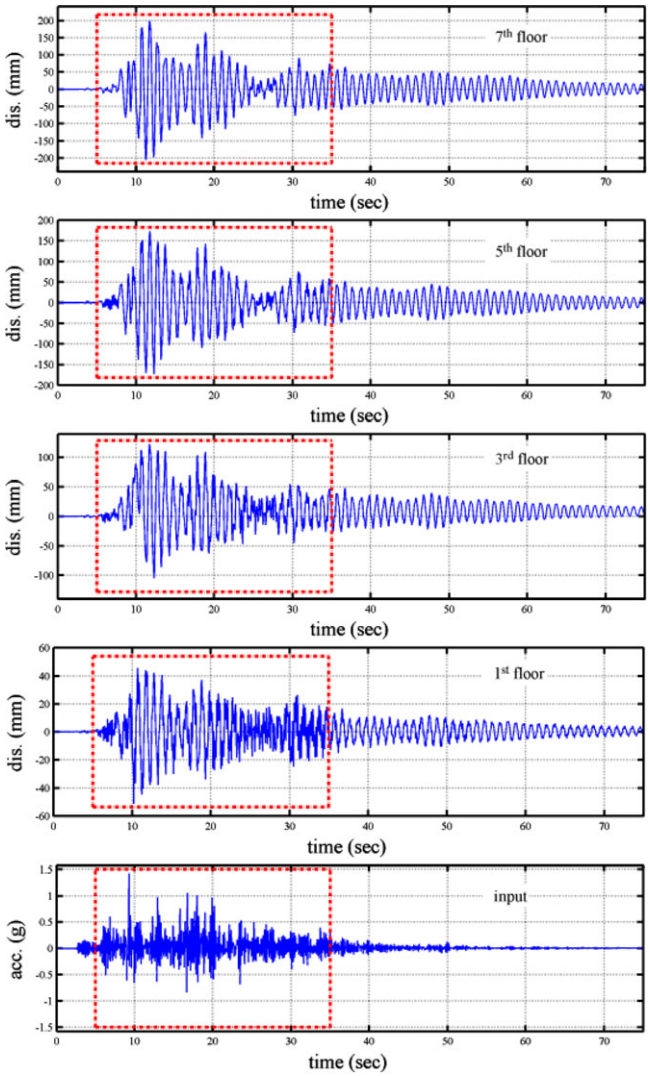

Fig. 11. Responses of frame under 1,200 gal of the Chi-Chi earthquake.

Notably, $\sqrt{k_n/m_n}$ (rad/s) is the theoretical natural frequency of the nth substructure and is identifiable by the MISO TVARX model established with an output of x_n^r and inputs of a_g and x_{n-1}. Consequently, $\sqrt{k_{n-1}/m_{n-1}}$ (rad/s), which is the theoretical natural frequency for the $(n-1)$th substructure, can be obtained through Equation (13). However, it is not able to identify the instantaneous modal damping ratio of the $(n-1)$th substructure.

The numerically simulated responses of the five-storey shear building with noise considered in Section 3 and the responses of the eight-storey steel fame under the shaking table tests considered in Section 4 were again processed to confirm the feasibility of the method for directly locating the damaged floors of a shear building under an earthquake based on variations of

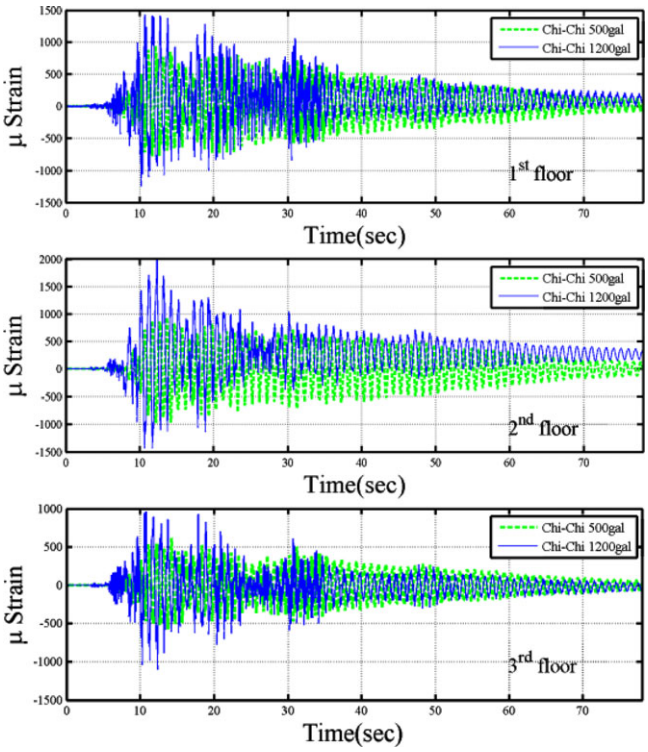

Fig. 12. Strain responses at columns of first, second, and third floor.

substructural instantaneous natural frequencies of the building over time. Excluding the damping ratio for the fourth floor, Figure 14 depicts the identified instantaneous natural frequencies and damping ratios for each substructure of the five-storey shear building. The instantaneous modal parameters of the second and third substructures (storeys) do not significantly change with time, and the identified frequencies and damping ratios differ from the actual values by less than 2% and 4%, respectively. The instantaneous modal parameters of the first, fourth, and fifth storeys vary periodically over time, and the identified instantaneous natural frequencies and damping ratios are different from the exact values by less than 2% and 20%, respectively.

Figure 15 illustrates the variations of the identified instantaneous natural frequencies and damping ratios of each substructure of the eight-storey steel frame under 500 and 1,200 gal of the Chi-Chi earthquake, except for the damping ratios for the seventh storey. When the frame was subjected to 500 gal of the Chi-Chi earthquake, no nonlinear behaviors were observed, and, as expected, the identified instantaneous natural frequencies of each storey do not significantly alter with time. The variations of natural frequencies with time are less than 0.2% of the mean values. In contrast, when the frame was subjected to 1,200 gal of the Chi-Chi earthquake, the instantaneous natural frequencies of the first to fourth storeys significantly change with time, but the instantaneous natural frequencies of the other storeys do not. The instantaneous natural frequencies and damping ratios of the first to fourth storeys clearly decrease and increase, respectively, at $t = 10$–12 seconds as the displacement responses of each floor gradually increase (see Figure 11). These results indicate that the stiffness of the first to fourth storeys significantly changed with time when the frame was under 1,200 gal of the Chi-Chi earthquake, and these storeys were somewhat damaged. Notably, Figure 12 shows the measurements obtained by strain gauges installed on the columns of the first to third stories, which also indicated that the columns yielded during such base excitation. This agreement indicates the practical applicability of this procedure to locate the possible damaged storeys of a real building with symmetry under a single severe earthquake.

6 CONCLUDING REMARKS

This work presented an approach to accurately determine the instantaneous modal parameters of a time-varying linear structure through a TVARX model. By expanding the time-dependent coefficient functions in a TVARX model with moving least-squares interpolation functions, a time-varying identification problem is transformed into a time invariant one. Continuous wavelet transform is further employed to the model to correctly identify the instantaneous modal parameters in the frequency ranges of interest. By incorporating a substructural technique, the proposed approach can accurately locate potentially damaged floors of a shear building subjected to an earthquake. The main advantages of the present procedure of locating the possibly damaged storeys are simple and no reference data (such as the data of the building without damage) needed. Certainly, an appropriate measuring system for substructures that are very susceptible to damage in a large earthquake should be carefully designed and installed in real applications.

A five-storey shear building under base excitation was numerically simulated to confirm the validity of the proposed approach for accurately determining the instantaneous modal parameters of the building and for locating the storeys with time-varying stiffness and damping. The numerically simulated shear building showed periodically time-varying stiffness and damping in the first, fourth, and fifth storeys. The numerical results clearly confirm that the approach indeed improves capability for using basis function expansion and regression approaches for accurately

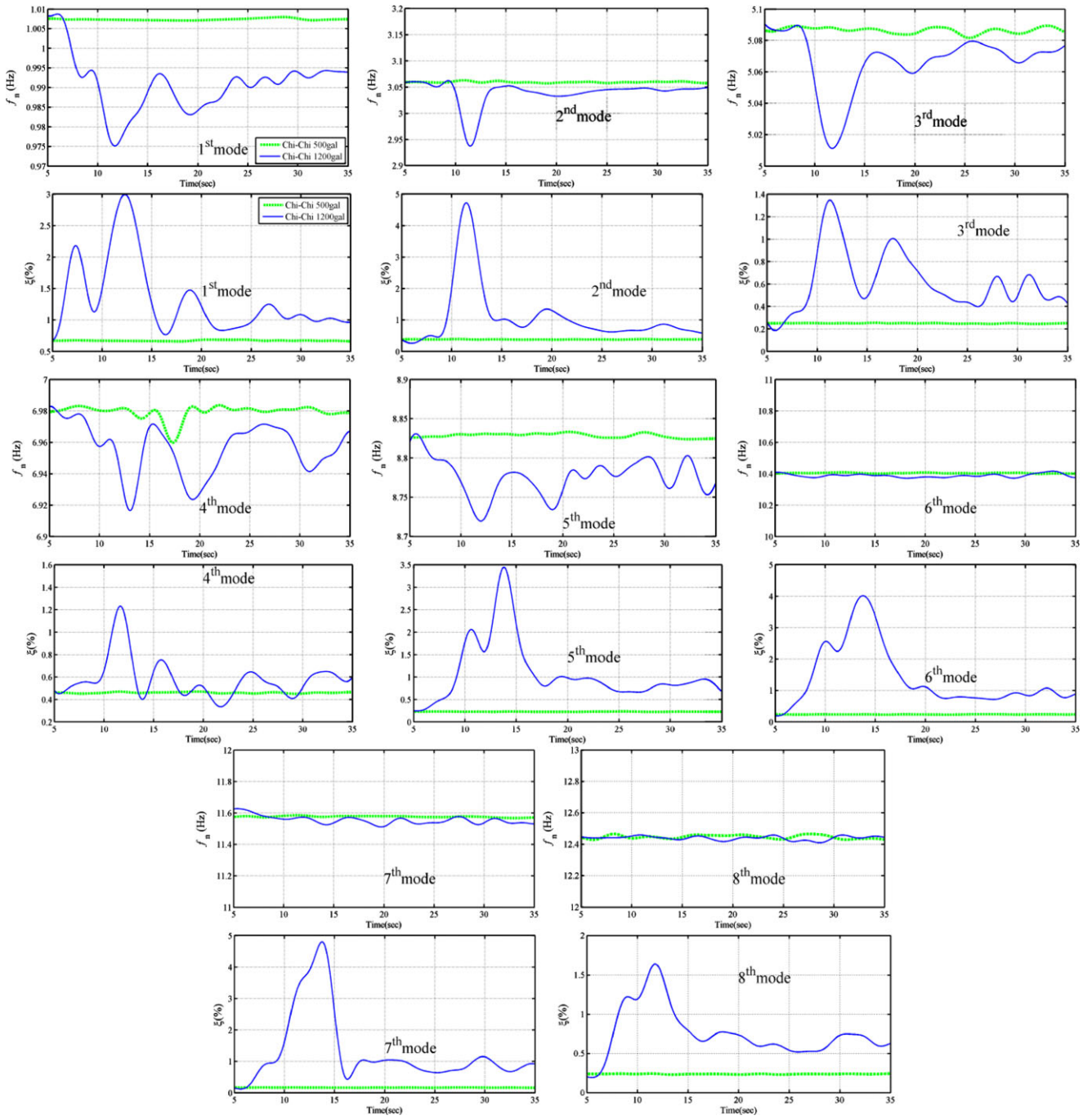

Fig. 13. Instantaneous modal parameters identified from the responses under 500 and 1,200 gal of the Chi-Chi earthquake.

determining the instantaneous modal parameters of a structure from noisy responses. The storeys with time-varying stiffness and damping and the behaviors of the stiffness and damping changing over time were easily located and determined from the identified substructural instantaneous natural frequencies and damping ratios.

The applicability of the proposed approach in processing the measured responses in a practical engineering was illustrated on an eight-storey steel frame, which is 1.8 m long, 1.2 m wide, and 8.5 m high, in shaking table tests. The frame behaved linearly and nonlinearly under 500 and 1,200 gal of the Chi-Chi earthquake, respectively. The identified instantaneous

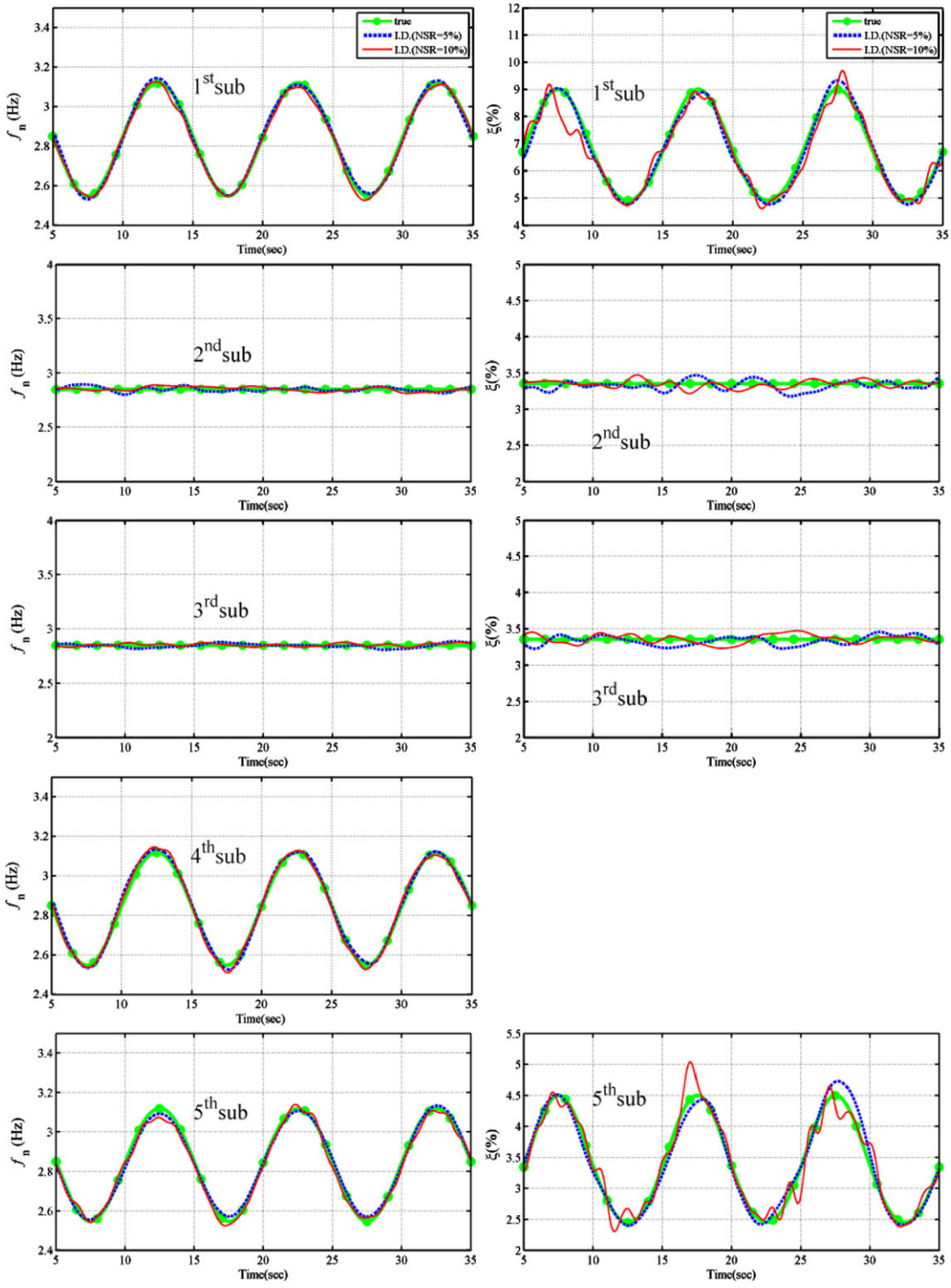

Fig. 14. Identified substructural instantaneous natural frequencies and damping ratios of a five-storey shear building.

natural frequencies and damping ratios of the full frame under the large base excitation significantly vary with time, while the identified instantaneous modal parameters for the small base excitation do not. Measured strain responses indicated that the columns of the first to third storeys yielded when the frame was under the large base excitation. The floors with yielding columns were correctly located from the identified substructural

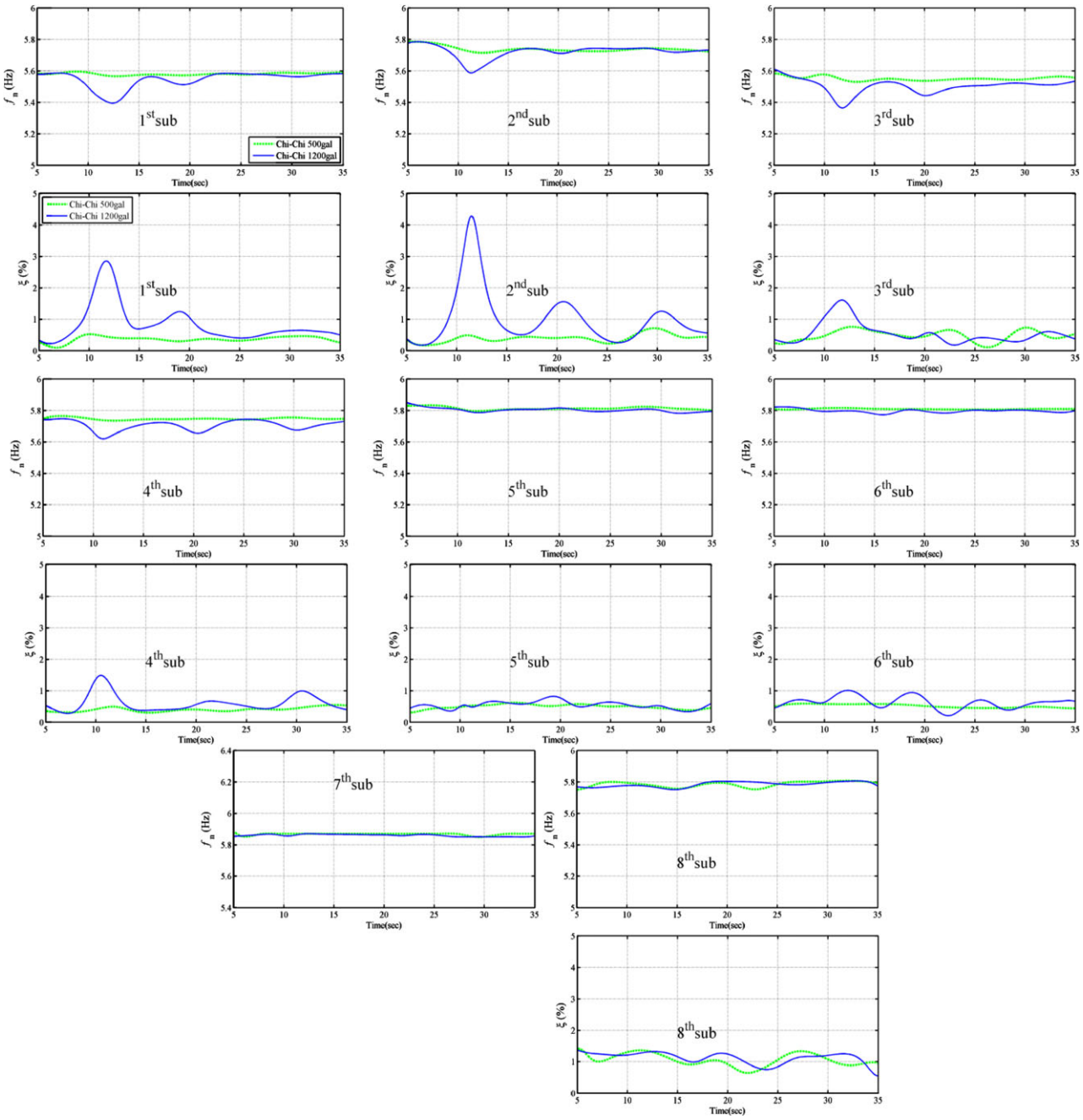

Fig. 15. Identified substructural instantaneous natural frequencies and damping ratios of an eight-storey steel frame.

instantaneous natural frequencies and damping ratios.

ACKNOWLEDGMENTS

The authors would like to thank the National Science Council of the Republic of China, Taiwan, for financially supporting this research under Contract No. NSC 100-2221-E-009-093-MY2. The appreciation is also extended to the National Center for Research on Earthquake Engineering for providing shaking table test data.

REFERENCES

Acharya, U. R., Vinitha Sree, S., Alvin, A. P. C. & Suri, J. S. (2012), Application of non-linear and wavelet based features for the automated identification of epileptic EEG

signals, *International Journal of Neural Systems*, **22**(2), 1250002–14.
Adeli, H., Gere, J. & Weaver, W., Jr. (1978), Algorithms for nonlinear structural dynamics, *Journal of Structural Division, ASCE*, **104**(ST2), 263–80.
Adeli, H. & Ghosh-Dastidar, S. (2004), Mesoscopic-wavelet freeway work zone flow and congestion feature extraction model, *Journal of Transportation Engineering, ASCE*, **130**(1), 94–103.
Adeli, H., Ghosh-Dastidar, S. & Dadmehr, N. (2008), A spatio-temporal wavelet-chaos methodology for EEG-based diagnosis of Alzheimer's disease, *Neuroscience Letters*, **144**(2), 190–94.
Adeli, H. & Jiang, X. (2006), Dynamic fuzzy wavelet neural network model for structural system identification, *Journal of Structural Engineering, ASCE*, **132**(1), 102–11.
Adeli, H. & Kim, H. (2004), Wavelet-hybrid feedback least mean square algorithm for robust control of structures, *Journal of Structural Engineering, ASCE*, **130**(1), 128–37.
Adeli, H. & Saleh, A. (1997), Optimal control of adaptive/smart bridge structures, *Journal of Structural Engineering*, **123**(2), 218–26.
Adeli, H. & Samant, A. (2000), An adaptive conjugate gradient neural network-wavelet model for traffic incident detection, *Computer-Aided Civil and Infrastructure Engineering*, **13**(4), 251–60.
Adewuyi, A.P. & Wu, Z. (2011), Vibration-based damage localization in flexural structures using normalized modal macrostrain techniques from limited measurements, *Computer-Aided Civil and Infrastructure Engineering*, **26**(3), 154–72.
Asutkar, V. G., Patre, B. M. & Basu, T. K. (2010), Identification of linear time-varying systems using haar basis functions, *International Journal of Information and Systems Sciences*, **6**(3), 333–44.
Belge, M. & Miller, E. L. (2000), A sliding window RLS-like adaptive algorithm for filtering alpha-stable noise, *IEEE Signal Processing Letters*, **7**(4), 86–89.
Bitaraf, M., Hurlebaus, S. & Barroso, L. R. (2012), Active and semi-active adaptive control for undamaged and damaged building structures under seismic load, *Computer-Aided Civil and Infrastructure Engineering*, **27**(1), 48–64.
Bocca, M., Mahmood, A., Eriksson, L. M., Kullaa, J. & Jäntti, R. (2011), A synchronized wireless sensor network for experimental modal analysis in structural health monitoring, *Computer-Aided Civil and Infrastructure Engineering*, **26**(7), 483–99.
Cho, B. H., Jo, J. S., Joo, S. J. & Kim, H. (2012), Dynamic parameter identification of secondary mass dampers based on full-scale tests, *Computer-Aided Civil and Infrastructure Engineering*, **27**(3), 218–30.
Choi, B. Y. & Bien, Z. (1989), Sliding-windowed weighted recursive least-squares method for parameter estimation, *Electron Letter*, **25**(20), 1381–82.
Cruz, P. J. S. & Salgado, R. (2009), Performance of vibration-based damage detection methods in bridges, *Computer-Aided Civil and Infrastructure Engineering*, **24**(1), 62–79.
Cusson, D., Lounis, Z. & Daigle, L. (2011), Monitoring life cycle performance of aging concrete highway bridges built in corrosive environments, *Computer-Aided Civil and Infrastructure Engineering*, **26**(7), 524–41.
Daubechies, I. (1988), Orthonormal basis of compactly supported wavelets, *Communication for Pure & Applied Mathematics*, **41**, 909–96.
Daubechies, I. (1992). *Ten Lectures on Wavelets*, Society for Industrial and Applied Mathematics, Philadelphia, PA.
Figueiredo, E., Park, G., Figueiras, J., Farrar, C. & Worden, K. (2011), Influence of the autoregressive model order on damage detection, *Computer-Aided Civil and Infrastructure Engineering*, **26**(3), 225–38.
Fortescue, T. R., Kershenbaum, L. S. & Ydstie, B. E. (1981), Implementation of self-tuning regulators with variable forgetting factors, *Automatica*, **17**(6), 831–5.
Gangone, M. V., Whelan, M. J. & Janoyan, K. D. (2011), Wireless monitoring of a multi-span bridge superstructure for diagnostic load testing and system identification, *Computer-Aided Civil and Infrastructure Engineering*, **26**(7), 560–79.
Gao, Y., Spencer, B. F., Jr. & Bernal, D. (2007), Experimental verification of the flexibility-based damage locating vector method, *Journal of Engineering Mechanics*, *ASCE*, **133**(10), 1043–49.
Ghosh-Dastidar, S. & Adeli, H. (2003), Wavelet clustering neural network model for freeway incident detection, *Computer-Aided Civil and Infrastructure Engineering*, **18**(5), 831–35.
Ghosh-Dastidar, S. & Adeli, H. (2006), Neural network-wavelet micro-simulation model for delay and queue length estimation at freeway work zones, *Journal of Transportation Engineering*, *ASCE*, **132**(4), 331–41.
Hazra, B., Sadhu, A., Roffel, A. J. & Narasimhan, S. (2012), Hybrid time-frequency blind source separation – towards ambient system identification of structures, *Computer-Aided Civil and Infrastructure Engineering*, **27**(5), 314–32.
Huang, C. S. (2001), Structural identification from ambient vibration measurement using the multivariate AR model, *Journal of Sound and Vibration*, **241**(3), 337–59.
Huang, C. S., Hung, S. L., Su, W. C. & Wu, C. L. (2009), Identification of time-variant modal parameters using TVARX and low-order polynomial function, *Computer-Aided Civil and Infrastructure Engineering*, **24**(7), 470–91.
Huang, C. S. & Su, W. C. (2007), Identification of modal parameters of a time invariant linear system by continuous wavelet transformation, *Mechanical System and Signal Processing*, **21**(4), 1642–64.
Jiang, X. & Adeli, H. (2004), Wavelet packet-autocorrelation function method for traffic flow pattern analysis, *Computer-Aided Civil and Infrastructure Engineering*, **19**(5), 324–37.
Jiang, X. & Adeli, H. (2005), Dynamic wavelet neural network for nonlinear identification of highrise buildings, *Computer-Aided Civil and Infrastructure Engineering*, **20**(5), 316–30.
Jiang, X. & Adeli, H. (2007), Pseudospectra, MUSIC, and dynamic wavelet neural network for damage detection of highrise buildings, *International Journal for Numerical Methods in Engineering*, **71**(5), 606–29.
Jiang, J. & Cook, R. (1992), Fast parameter tracking RLS algorithm with high noise immunity, *Electron Letter*, **28**(22), 2042–45.
Jiang, X., Ma, Z. J. & Ren, W. X. (2012), Crack detection from the slope of the mode shape using complex continuous wavelet transform, *Computer-Aided Civil and Infrastructure Engineering*, **27**(3), 187–201.
Jiang, X., Mahadevan, S. & Adeli, H. (2007), Bayesian wavelet packet denoising for structural system identification, *Structural Control and Health Monitoring*, **14**(2), 333–56.
Kang, N., Kim, H., Choi, S., Jo, S., Hwang, J. S. & Yu, E. (2012), Performance evaluation of TMD under typhoon

using system identification and inverse wind load estimation, *Computer-Aided Civil and Infrastructure Engineering*, **27**(6), 455–73.

Karim, A. & Adeli, H. (2003), Fast automatic incident detection on urban and rural freeways using the wavelet energy algorithm, *Journal of Transportation Engineering*, *ASCE*, **129**(1), 57–68.

Kim, H. & Adeli, H. (2005a), Hybrid control of smart structures using a novel wavelet-based algorithm, *Computer-Aided Civil and Infrastructure Engineering*, **20**(1), 7–22.

Kim, H. & Adeli, H. (2005b), Wavelet hybrid feedback-LMS algorithm for robust control of cable-stayed bridges, *Journal of Bridge Engineering*, *ASCE*, **10**(2), 116–23.

Kim, H. & Adeli, H. (2005c), Wind-induced motion control of 76-story benchmark building using the hybrid damper-tuned liquid column damper system, *Journal of Structural Engineering*, *ASCE*, **131**(12), 1794–802.

Lancaster, P. & Šalkauskas, K. (1990), *Curve and Surface Fitting—An Introduction*, Academic Press, NY.

Leung, S. H. & So, C. F. (2005), Gradient-based variable forgetting factor RLS algorithm in time-varying environments, *IEEE Transactions on Signal Processing*, **53**(8), 3141–50.

Li, Y. & Wei, H. L. & Billings, S. A. (2011), Identification of time-varying systems using multi-wavelet basis functions, *IEEE Transactions on Control System Technology*, **19**(3), 656–63.

Lin, C. M., Ting, A. B., Hsu, C. F. & Chung, C. M. (2012), Adaptive control for MIMO uncertain nonlinear systems using recurrent wavelet neural network, *International Journal of Neural Systems*, **22**(1), 37–50.

Liu, G. R. (2003), *Mesh Free Methods: Moving Beyond the Finite Element Method*, CRC Press, NY.

Ljung, L. (1987), *System Identification, Theory for the User*, Prentice-Hall, Englewood Cliffs, NJ.

Ljung, L. & Gunnarsson, S. (1990), Adaptation and tracking in system identification—a survey, *Automatica*, **26**(1), 7–21.

Loh, C. H., Lin, C. Y. & Huang, C. C. (2000), Time domain identification of frames under earthquake loadings, *Journal of Engineering Mechanics*, *ASCE*, **126**(7), 693–703.

Marano, G. C., Quaranta, G. & Monti, G. (2011), Modified genetic algorithm for the dynamic identification of structural systems using incomplete measurements, *Computer-Aided Civil and Infrastructure Engineering*, **26**(2), 92–110.

Marmarelis, V. Z. (1987), *Advanced Methods of Physiological System Modeling*, University of Southern California, Los Angeles.

Moaveni, B., Conte, J. P. & Hemez, F. M. (2009), Uncertainty and sensitivity analysis of damage identification results obtained using finite element model updating, *Computer Aided Civil and Infrastructure Engineering*, **24**(5), 320–34.

Morbidi, F., Farulli, A., Orattichizzo, D., Rizzo, C. & Rossi, S. (2008), Application of Kalman filter to remove TMS-induced artifacts from EEG recordings, *IEEE Transactions on Control System Technology*, **16**(6), 1360–6.

Moser, P. & Moaveni, B. (2011), Environmental effects on the identified natural frequencies of the Dowling Hall Footbridge, *Mechanical System and Signal Processing*, **25**(7), 2336–57.

Niedźwiecki, M. (1988), Functional series modelling approach to identification of nonstationary stochastic systems, *IEEE Transactions on Automatic Control*, **33**, 955–61.

Niedźwiecki, M. (2000), *Identification of Time-Varying Processes*, John Wiley & Sons, NY.

Nishikawa, T., Fujino, Y., Yoshida, J. & Sugiyama, T. (2012), Concrete crack detection by multiple sequential image filtering, *Computer-Aided Civil and Infrastructure Engineering*, **27**(1), 29–47.

Osornio-Rios, R. A., Amezquita-Sanchez, J. P., Romero-Troncoso, R. J. & Garcia-Perez, A. (2012), MUSIC-neural network analysis for locating structural damage in truss-type structures by means of vibrations, *Computer-Aided Civil and Infrastructure Engineering*, **27**(9), 687–98.

Pandey, A. K. & Biswas, M. (1994), Damage detection in structures using changes in flexibility, *Journal of Sound and Vibration*, **169**(1), 3–17.

Park, D. J. & Jun, B. E. (1992), Self-perturbing recursive least squares algorithm with fast tracking capability, *Electron Letter*, **28**(6), 558–59.

Park, H. S., Lee, H. M., Adeli, H. & Lee, I. (2007), A new approach for health monitoring of structures: terrestrial laser scanning, *Computer-Aided Civil and Infrastructure Engineering*, **22**(1), 19–30.

Patjawit, A. & Knaok-Nukulchai, W. (2005), Health monitoring of highway bridges based on a global flexibility index, *Engineering Structures*, **27**(9), 1385–91.

Poulimenos, A. G. & Fassois, S. D. (2006), Parametric time-domain methods for non-stationary random vibration modelling and analysis – a critical survey and comparison, *Mechanical Systems and Signal Processing*, **20**, 763–816.

Poulimenos, A. G. & Fassois, S. D. (2009), Output-only stochastic identification of a time-varying structure via functional series TARMA models, *Mechanical Systems and Signal Processing*, **23**(4), 1180–204.

Qiao, L., Esmaeily, A. & Melhem, H. G. (2012), Signal pattern-recognition for damage diagnosis in structures, *Computer-Aided Civil and Infrastructure Engineering*, **27**(9), 699–710.

Raich, A. M. & Liszkai, T. R. (2012), Multi-objective optimization of sensor and excitation layouts for frequency response function-based structural damage identification, *Computer-Aided Civil and Infrastructure Engineering*, **27**(2), 95–117.

Sampaio, P. R. C., Maia, N. M. M. & Silva, J. M. M. (1999), Damage detection using the frequency response-function curvature method, *Journal of Sound and Vibration*, **226**(5), 1029–42.

Schoefs, F., Yáñez-Godoy, H. & Lanata, F. (2011), Polynomial chaos representation for identification of mechanical characteristics of instrumented structures, *Computer-Aided Civil and Infrastructure Engineering*, **26**(3), 173–89.

Sohn, H., Dzwonczyk, M. J., Straser, E. G., Kiremidjian, A. S., Law, K. H. & Meng, T. H. (1999), An experimental study of temperature effect on modal parameters of the Alamosa Canyon Bridge. *Earthquake Engineering and Structural Dynamics*, **28**(8), 879–97.

Stratman, B., Mahadevan, S., Li, C. & Biswas, G. (2011), Identification of critical inspection samples among railroad wheels by similarity-based agglomerative clustering, *Integrated Computer-Aided Engineering*, **18**(3), 203–19.

Su, W. C. (2008), Identification of modal parameters of structures via time series models, Ph.D. dissertation, National Chiao Tung University, Hsinchu, Taiwan.

Su, W. C., Huang, C. S., Hung, S. L., Chen, L. J. & Lin, W. J. (2012), Damage diagnosis to a shear building based on its sub-structural natural frequencies, *Engineering Structures*, **39**, 126–38.

Talebinejad, I., Fischer, C. & Ansari, F. (2011), Numerical evaluation of vibration based methods for damage assessment of cable stayed bridges, *Computer-Aided Civil and Infrastructure Engineering*, **26**(3), 239–51.

Theodoridis, D., Boutalis, Y. & Christodoulou, M. (2012), Dynamical recurrent neuro-fuzzy identification schemes employing switching parameter hoping, *International Journal of Neural Systems*, **22**(2), 1250004–16.

Toplis, B. & Pasupathy, S. (1988), Tracking improvements in fast RLS algorithm using a variable forgetting factor, *IEEE Transactions on Acoustics Speech Signal Processing*, **36**(2), 206–27.

Tsatsanis, M. K. & Giannakis, G. B. (1993), Time-varying system identification and model validation using wavelets, *IEEE Transactions Signal Processing*, **41**, 3512–23.

Wei, H. L., Billings, S. A. & Liu, J. (2010), Time-varying parametric modeling and time-dependent spectral characterization with application to EEG signal using multiwavelets, *International Journal of Modelling, Identification and Control*, **9**(3), 215–25.

Wood, M. G. (1992), Damage analysis of bridge structures using vibration techniques, Ph.D. dissertation, University of Aston, Birmingham, Birmingham, UK.

Xia, Y., Ni, Y. Q., Zhang, P., Liao, W. Y. & Ko, J. M. (2011), Stress development of a super-tall structure during construction: numerical analysis and field monitoring verification, *Computer-Aided Civil and Infrastructure Engineering*, **26**(7), 542–59.

Xiang, J. & Liang, M. (2012), Wavelet-based detection of beam cracks using modal shape and frequency measurements, *Computer-Aided Civil and Infrastructure Engineering*, **27**(6), 439–54.

Yan, W. J. & Ren, W. X. (2012), Operational modal parameter identification from power spectrum density transmissibility, *Computer-Aided Civil and Infrastructure Engineering*, **27**(3), 202–17.

Yuen, K. V. & Katafygiotis, L. S. (2006), Substructure identification and health monitoring using response measurement only, *Computer-Aided Civil and Infrastructure Engineering,* **21**(4), 280–91.

Zheng, Y., Lin, Z. & Tay, D. B. H. (2001), Time-varying parametric system multiresolution identication by wavelets, *International Journal of Systems Science*, **32**(6), 775–93.

Zhou, Z. & Adeli, H. (2003), Time-frequency signal analysis of earthquake records using Mexican hat wavelets, *Computer-Aided Civil and Infrastructure Engineering*, **18**(5), 379–89.

Zou, R., Wang, H. & Chon, K. H. (2003), A robust time-varying identification algorithm using basis functions, *Annals of Biomedical Engineering*, **31**, 840–53.

APPENDIX

Using polynomial basis functions to express $\phi_{kl}^i(t)$ yields

$$\phi_{kl}^i(t) = \sum_{n=0}^{\bar{N}} \bar{a}_{kln}^i t^n = \mathbf{p}^T \mathbf{a}_{kl}^i \tag{A.1}$$

where $\mathbf{p}^T = (1, t, t^2, \ldots, t^{\bar{N}})$, $(\mathbf{a}_{kl}^i)^T = (\bar{a}_{kl0}^i, \bar{a}_{kl1}^i, \bar{a}_{kl2}^i, \ldots, \bar{a}_{kl\bar{N}}^i)$ and $\bar{a}_{kln}^i$ are the coefficients to be determined. A weighted least-squares technique is applied to determine coefficients $\bar{a}_{kln}^i$ in Equation (A.1). Let $\bar{\phi}_{kln}^i$ represent the true value of $\phi_{kl}^i(t_n)$. Vector $\mathbf{a}_{kl}^i$ is determined by minimizing the error function defined by

$$E(t) = \sum_{n=1}^{\bar{l}} w(t, t_n)\left(\mathbf{p}^T(t_n)\mathbf{a}_{kl}^i - \bar{\boldsymbol{\phi}}_{kln}^i\right)^2 \tag{A.2}$$

where $w(t, t_n)$ is a weight function that must be positive, and $\bar{l}$ is the number of nodal points for $\phi_{kl}^i(t)$. Minimizing E yields

$$\frac{\partial E}{\partial \mathbf{a}_{kl}^i} = \mathbf{0} \tag{A.3}$$

Solving for $\mathbf{a}_{kl}^i$ from Equation (A.3) and substituting it into Equation (A.1) gives $\phi_{kl}^i(t) = \boldsymbol{\varphi}(t)\bar{\boldsymbol{\phi}}_{kl}^i$, where $\bar{\boldsymbol{\phi}}_{kl}^i = (\bar{\phi}_{kl1}^i, \bar{\phi}_{kl2}^i, \ldots, \bar{\phi}_{kl\bar{l}}^i)^T$.